

Microstructured chalcogenide optical fibers from As₂S₃ glass: towards new IR broadband sources

M. El-Amraoui,¹ G. Gadret,¹ J. C. Jules,¹ J. Fatome,¹ C. Fortier,¹ F. Désévéday,¹
I. Skripatchev,² Y. Messaddeq,² J. Troles,³ L. Brilland,⁴ W. Gao,⁵ T. Suzuki,⁵
Y. Ohishi,⁵ and F. Smektala^{1,*}

¹ ICB Laboratoire Interdisciplinaire Carnot de Bourgogne, UMR 5209 CNRS-Université de Bourgogne, Av. A. Savary, 21078 Dijon, France.

² Institute of Chemistry – UNESP, P.O. Box 355, Araraquara, SP 14801-970, Brazil.

³ Sciences Chimiques de Rennes, UMR 6226 CNRS-Université de Rennes I, 35042 Rennes Cedex, France

⁴ PERFOS, 11, rue Louis de Broglie, 22300 Lannion, France

⁵ Research Center for Advanced Photon Technology, Toyota Technological Institute, 2-12-1, Hisakata, Tempaku, Nagoya 468-8511, Japan.

*frederic.smektala@u-bourgogne.fr

Abstract: The aim of this paper is to present an overview of the recent achievements of our group in the fabrication and optical characterizations of As₂S₃ microstructured optical fibers (MOFs). Firstly, we study the synthesis of high purity arsenic sulfide glasses. Then we describe the use of a versatile process using mechanical drilling for the preparation of preforms and then the drawing of MOFs including suspended core fibers. Low losses MOFs are obtained by this way, with background level of losses reaching less than 0.5 dB/m. Optical characterizations of these fibers are then reported, especially dispersion measurements. The feasibility of all-optical regeneration based on a Mamyshev regenerator is investigated, and the generation of a broadband spectrum between 1 μm and 2.6 μm by femto second pumping around 1.5 μm is presented.

©2010 Optical Society of America

OCIS codes: (060.2390) Fiber optics, infrared; (060.5295) Photonic crystal fibers; (190.4370) Nonlinear optics, fibers; (160.4330) Nonlinear optical materials; (160.2750) Glass and other amorphous materials; (060.2280) Fiber design and fabrication; (060.2270) Fiber characterization.

References and links

1. J. C. Knight, T. A. Birks, P. St. J. Russell, and D. M. Atkin, "All-silica single-mode optical fiber with photonic crystal cladding," *Opt. Lett.* **21**(19), 1547–1549 (1996).
2. G. P. Agrawal, *Application of nonlinear fiber optics*, Academic Press, Boston (2001).
3. P. St. J. Russell, "Photonic crystal fibers," *Science* **299**(5605), 358–362 (2003).
4. J. C. Knight, "Photonic crystal fibres," *Nature* **424**(6950), 847–851 (2003).
5. F. Smektala, C. Quémard, L. LeNeindre, J. Lucas, A. Barthélémy, and C. De Angelis, "Chalcogenide glasses with large non-linear refractive indices," *J. Non-Cryst. Solids* **239**(1-3), 139–142 (1998).
6. F. Smektala, C. Quémard, V. Couderc, and A. Barthélémy, "Non-linear optical properties of chalcogenide glasses measured by Z-scan," *J. Non-Cryst. Solids* **274**(1-3), 232–237 (2000).
7. T. M. Monro, Y. D. West, D. W. Hewak, N. G. R. Broderick, and D. J. Richardson, "Chalcogenide holey fibres," *Electron. Lett.* **36**(24), 1998–2000 (2000).
8. F. Désévéday, G. Renversez, L. Brilland, P. Houizot, J. Troles, Q. Coulombier, F. Smektala, N. Traynor, and J. L. Adam, "Small-core chalcogenide microstructured fibers for the infrared," *Appl. Opt.* **47**(32), 6014–6021 (2008).
9. F. Smektala, F. Désévéday, L. Brilland, P. Houizot, J. Troles, and N. Traynor, "Advances in the elaboration of chalcogenide photonic crystal fibers for the mid infrared," *SPIE* **6588**, 58803 (2007).
10. J. S. Sanghera, L. B. Shaw, and I. D. Aggarwal, "Chalcogenide Glass-Fiber-Based Mid-IR Sources and Applications," *IEEE J. Sel. Top. Quantum Electron.* **15**(1), 114–119 (2009).
11. X. Feng, A. K. Mairaj, D. W. Hewak, and T. M. Monro, "Non silica Glasses for Holey Fibers," *J. Lightwave Technol.* **23**(6), 2046–2053 (2005).

12. R. Frerichs, "New optical glasses with good transparency in the infrared," *J. Opt. Soc. Am.* **43**(12), 1153–1157 (1953).
13. J. A. Savage, "Optical properties of chalcogenide glasses," *J. Non-Cryst. Solids* **47**(1), 101–115 (1982).
14. S. Shibata, T. Manabe, and M. Horiguchi, "Preparation of Ge-S Glass Fibers with Reduced OH, SH Content," *Jpn. J. Appl. Phys.* **20**(1), 13–16 (1981).
15. C. T. Moynihan, P. B. Macedo, N. S. Maklad, R. Mohr, and R. Howard, "Intrinsic and impurity infrared absorption in As-Se glass," *J. Non-Cryst. Solids* **17**(3), 369–385 (1975).
16. S. Shibata, Y. Terunuma, and T. Manabe, "Sulfide glass fibers for infrared transmission," *Mater. Res. Bull.* **16**(6), 703–714 (1981).
17. G. G. Devyatikh, E. M. Dianov, V. G. Plotnichenko, I. V. Scripachev, and M. F. Churbanov, "Fiber waveguides from high purity chalcogenide glass," *Russ. High Purity Substances J.* **1**, 7–36 (1991).
18. D. L. Wood, and J. Tauc, "Weak absorption tails in amorphous semiconductors," *Phys. Rev. B* **5**(8), 3144–3151 (1972).
19. M. F. Churbanov, "High purity chalcogenide glasses as materials for fiber optics," *J. Non-Cryst. Solids* **184**, 25–29 (1995).
20. G. G. Devyatikh, M. F. Churbanov, I. V. Scripachev, G. E. Snopatin, E. M. Dianov, V. G. Plotnichenko, "Recent developments in As-S glass fibres," *J. of Non-Cryst. Solids* **256&257**, 318–22 (1999).
21. M. F. Churbanov, I. V. Scripachev, G. E. Snopatin, V. S. Shiryaev, and V. G. Plotnichenko, "High purity glasses based on arsenic chalcogenides," *J. Optoelectron. Adv. Mater.* **3**, 341–349 (2001).
22. G. E. Snopatin, M. F. Churbanov, A. A. Pushkin, V. V. Gerasimenko, E. M. Dianov, and V. G. Plotnichenko, "High purity arsenic-sulfide glasses and fibers with minimum attenuation of 12 dB/km," *Optoelectron. Adv. Mater. Rapid Commun.* **3**(7), 669–671 (2009).
23. M. C. J. Large, L. Poladian, G. Barton, and M. Eijkelenborg, "Microstructured polymer optical fibers", Springer (2008).
24. M. R. E. Lamont, B. Luther-Davies, D. Y. Choi, S. Madden, and B. J. Eggleton, "Supercontinuum generation in dispersion engineered highly nonlinear ($\gamma = 10$ /W/m) As_2S_3 chalcogenide planar waveguide," *Opt. Express* **16**(19), 14938–14944 (2008).
25. G. Boudebs, F. Sanchez, J. Troles, and F. Smektala, "Nonlinear optical properties of chalcogenide glasses: comparison between Mach-Zehnder interferometry and Z-scan techniques," *Opt. Commun.* **199**(5-6), 425–433 (2001).
26. V. G. Borisevich, V. G. Plotnichenko, I. V. Scripachev, and M. F. Churbanov, "Extension coefficient of SH groups in vitreous arsenic sulphide," *Russ. High Purity Substances J.* **4**, 759–762 (1990).
27. L. Brilland, J. Troles, P. Houizot, F. Désévéday, Q. Coulombier, G. Renversez, T. Chartier, T. N. Nguyen, J.-L. Adam, and N. Traynor, "Interfaces impact on the transmission of chalcogenides photonic crystal fibres," *J. Ceram. Soc. Jpn.* **116**(1358), 1024–1027 (2008).
28. J. Troles, L. Brilland, F. Smektala, P. Houizot, F. Désévéday, Q. Coulombier, N. Traynor, T. Chartier, T. N. Nguyen, J. L. Adam, and G. Renversez, "Chalcogenide Microstructured Fibers for Infrared Systems, Elaboration Modelization, and Characterization," *Fiber Inter. Opt.* **28**(1), 11–26 (2009).
29. M. El-Amraoui, J. Fatome, J. C. Jules, B. Kibler, G. Gadret, C. Fortier, F. Smektala, I. Skripachev, C. F. Polacchini, Y. Messaddeq, J. Troles, L. Brilland, M. Szpulak, and G. Renversez, "Strong infrared spectral broadening in low-loss As-S chalcogenide suspended core microstructured optical fibers," *Opt. Express* **18**(5), 4547–4556 (2010).
30. J. Fatome, C. Fortier, T. N. Nguyen, T. Chartier, F. Smektala, K. Messaad, B. Kibler, S. Pitois, G. Gadret, C. Finot, J. Troles, F. Desevedavy, P. Houizot, G. Renversez, L. Brilland, and N. Traynor, "Linear and Nonlinear Characterizations of Chalcogenide Photonic Crystal Fibers," *J. Lightwave Technol.* **27**(11), 1707–1715 (2009).
31. M. Szpulak, and S. Février, "Chalcogenide As_2S_3 Suspended Core Fiber for Mid-IR Wavelength Conversion Based on Degenerate Four-Wave Mixing," *IEEE Photon. Technol. Lett.* **21**(13), 884–886 (2009).
32. P. V. Mamyshev, "All-optical data regeneration based on self-phase modulation effect," *Proc. European Conference on Optical Communication, ECOC* **98**, 475–476 (1998).
33. L. Fu, M. Rochette, V. Ta'eed, D. Moss, and B. Eggleton, "Investigation of self-phase modulation based optical regeneration in single mode As_2Se_3 chalcogenide glass fiber," *Opt. Express* **13**(19), 7637–7644 (2005).
34. L. A. Provost, C. Finot, P. Petropoulos, K. Mukasa, and D. J. Richardson, "Design scaling rules for 2R-optical self-phase modulation-based regenerators," *Opt. Express* **15**(8), 5100–5113 (2007).
35. C. Finot, T. N. Nguyen, J. Fatome, T. Chartier, L. Bramerie, M. Gay, S. Pitois, and J. C. Simon, "Numerical study of an optical regenerator exploiting self-phase modulation and spectral offset filtering at 40 Gbit/s," *Opt. Commun.* **281**(8), 2252–2264 (2008).
36. M. Liao, C. Chaudhari, G. Qin, X. Yan, T. Suzuki, and Y. Ohishi, "Tellurite microstructure fibers with small hexagonal core for supercontinuum generation," *Opt. Express* **17**(14), 12174–12182 (2009).

1. Introduction

Proposed for the first time in early 90's by J. C. Knight [1], photonic crystal fibers, also called microstructured or holey fibers, have led to a huge research effort all over the world due to its innovative properties compared to the traditional standard fibers. The potential applications,

starting with telecommunications, now extend to spectroscopy, metrology, microscopy, astronomy, micromachining, biology and sensing [2–4].

The main background materials of the researched MOFs are oxide based glasses, including silica and heavy oxide glasses. However, since the latter are not transparent at wavelengths longer than $\sim 6 \mu\text{m}$, it appears necessary to consider alternative glasses for particular applications. It is well known that chalcogenide glasses exhibit high transparency in the mid-IR region (10–20 μm) together with high refractive index ($n = 2.0 - 3.5$) and high non linearity [5]. Consequently, this class of materials gathers good candidates for applications, and particularly for nonlinear optics, in this spectral range [5,6].

Compared to oxide based glasses, the synthesis of chalcogenide glasses is more complicated to control, due to their lower chemical stability. Although the first chalcogenide glass MOF has been already fabricated in 2000 [7], the research works did not allow yet to meet the applications requirements. In fact only a few research groups have reported consistent results, in which two main techniques have been used to fabricate chalcogenide glass MOFs. The first one is the capillary-stacking technique, which is the most commonly used to manufacture silica MOFs, and which is also widely used for chalcogenide glass MOFs fabrication [8–10]. The main advantage of this technique is the ability to manufacture microstructured preforms with highly complex periodic geometry (> 60 holes), but this necessitates a huge amount of tricky handling. The second one is the extrusion technique, which seems simpler than the stack and draw one, but which is still quite challenging when aiming for fabrication of preforms with very complex microstructure pattern, like the triangular holey structure with more than three rings of holes [11].

In this paper, we demonstrate the fabrication of di-arsenic tri-sulfide (As_2S_3) glass MOFs using a mechanical drilling we have developed. According to this, we can manufacture preforms with various microstructures from simple ones to more complex ones. This process appears quite promising in view of a large-scale production of chalcogenide MOFs. These fibers would be the base for the fabrication of optical amplifiers, chemical sensors, laser radiation transmission devices, IR fiber radiometers and for the development of new non-linear fiber optics such as for example new supercontinuum sources exhibiting broadband generation in the infrared spectral range above 2 μm .

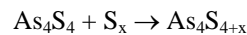
2. Preparation of As_2S_3 glass, preforms and microstructured fibers

2.1 Preparation of As_2S_3 glass

The usual technique used for As_2S_3 glass preparation is a solidification of the glass batch after melting of pristine elemental substances. Basically, initial elements arsenic (As) and sulfur (S) are placed under vacuum into a sealed silica ampoule and then heated up to 700–800 $^\circ\text{C}$ for several tens of hours. Frerichs in 1953 used distillation for the first time in order to improve the optical quality of vitreous As_2S_3 . He measured a good resulting transparency for As_2S_3 glass in the infrared and explained it [12]. It is well known that carbon, oxides and hydrogenous impurities give a high contribution to the absorption of light in the near infrared range. The main impurities absorption bands in As-S glasses are given in [13–17]. In [18], influence of metal impurities on the As-S glasses absorption in the so called “weak absorption tail range” was studied. Thus, the precursors used for synthesis of high purity chalcogenide glasses must have low content of carbon, oxides and hydrogenous impurities. In the case of arsenic, oxygen presents in the raw material is chemically combined and forms arsenic oxides. Carbon is usually presents in As in the form of micro inclusions whose size lies from 0.05 μm up to 0.2 μm , with a concentration in commercial high purity arsenic (5N) reaching 10^7 – 10^8 cm^{-3} [19–21]. Then, sublimation is conventionally used for arsenic purification. But the efficiency of this technique is low indeed. At standard evaporation rates an accumulation of carbon particles takes place at the surface of the sublimed arsenic [20]. To improve this efficiency, we have tried a very low sublimation rate, which must not exceed $10^{-6} \text{ cm}^3/\text{cm}^2 \cdot \text{s}$.

However, this low evaporation rate leads to an increasing arsenic/silica ampoule contact time, provoking further contamination of purified arsenic. Moreover, even for the usual amount of material needing to be purified in the lab (~0.1 kg/synthesis campaign) such low evaporation rates are not really acceptable.

These different works show clearly that another approach is necessary for the preparation of high purity As_2S_3 glass. For that purpose, arsenic mono-sulfide (As_4S_4) can be chosen as a starting material, instead of arsenic. Indeed, arsenic mono-sulfide seems to be a suitable compound in terms of distillation under vacuum and purification efficiency [20]. In the solid state, it is a polycrystalline compound that does not form neither glass nor polymer when heated at temperatures higher than the melting one ($T_{\text{melting}} = 320\text{ }^\circ\text{C}$) and then cooled. The melt of As_4S_4 is a low viscosity liquid whose viscosity is comparable to this of water. This property is interesting since it is one of the main conditions to increase the efficiency of melted liquids purification. After preliminary purification of As_4S_4 by distillation under vacuum, high purity arsenic sulfide glasses can thus be prepared using the following reaction [20]:



By adding suitable quantities of pure sulfur, various vitreous compositions of As_xS_y glasses can be prepared. This technique of pure As-S glass preparation was worked out for the first time in 1972 [18]. It led to the design of optical fibers whose losses were 23 dB/km at 2.4 μm . At the present time, optical losses of As-S fibers have been reduced to 12 dB/km at 3 μm [22].

Thus, according to above mentioned process, we have prepared pure As_2S_3 glass using preliminary purification of the intermediate compound As_4S_4 . Synthesis of As_4S_4 is carried out in static conditions without mechanical mixing of the melt. Mixing and homogenization of As_4S_4 melt is effective because of the low viscosity of its melt and the convection in the liquid. The temperature of As_4S_4 synthesis does not exceed 450 $^\circ\text{C}$. The duration of the synthesis is from 8 to 10 hours. Sulfur added to batch has been also preliminary purified by heating under vacuum, using temperature near melting point (~120 $^\circ\text{C}$) during several hours. After melting of high purity As_2S_3 glass, cylindrical preforms are prepared by ordinary cooling of the liquid batch. The resulting cylinders are then annealed in a conventional way in order to remove mechanical strains which could lead to glass breakdown during the MOF preform mechanical shaping step.

2.2 Preforms and microstructured fibers elaboration

We have developed a mechanical drilling for the preparation of preforms with a variety of geometrical patterns in view of MOFs drawing. It consists to drill holes in a chalcogenide glass rod. Some drilling techniques have been previously successfully used to prepare preforms such as for example ultrasonic drilling for glasses [11] or mechanical drilling for polymer [23]. We have here applied a mechanical drilling to chalcogenide glasses which is to our knowledge original. The position of the holes must be precisely controlled, as well as the friction between the glass and the tool to avoid an increasing of the temperature of the glass and its eventual fusion. The quality of the inner surface of the holes is also critical for the quality of the subsequently drawn fiber. By optimisation of the drilling parameters, especially rotation speed and applied force, these requirements can be reached. The drilling of a regular pattern of holes in a glass rod is thus possible, with quite thin matter bridges between the holes.

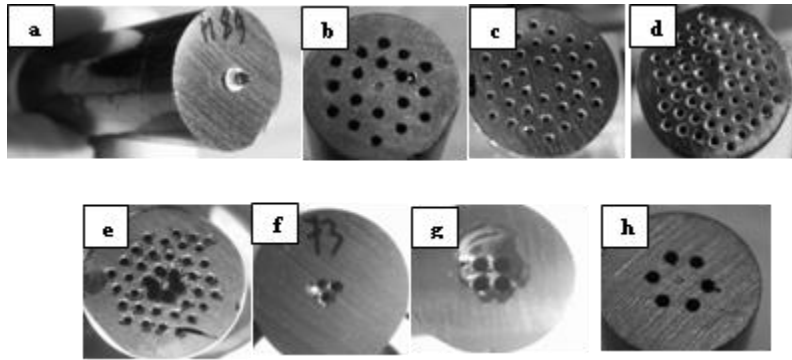


Fig. 1. Pictures of 16 mm outer diameter preforms elaborated by mechanical drilling. Preform for core clad fiber (a: 1 hole); Preforms for microstructured fibers (b: 2 rings/18 holes; c: 3 rings/36 holes; d: 4 rings/64 holes; e: 3 rings/34 holes + 2 big holes); Preforms for suspended core fibers (f: 3 holes, g: 4 holes, h: 6 holes).

We prepared this way versatile patterned preforms such as a simple rods intended to mono-index fiber drawing, preforms for standard core clad fibers, preforms devoted to “traditional” microstructured fibers with several rings of holes in a triangular pattern (eighteen holes, thirty six holes and sixty four holes), preforms for other microstructured fibers profiles with various numbers of holes and preforms for suspended core fibers with three, four or six holes around a solid core. For all these preforms the outer diameter is 16 mm, the diameter d of holes is equal to 0.8 mm and their length to about 30 mm. For the microstructured fibers where this parameter is pertinent, the ratio $d/\Lambda = 0.4$ was respected by leaving a distance equal to $\Lambda = 2$ mm between two neighboring holes. Figure 1 collects some pictures of the obtained preforms.

Many parameters are controlled during MOFs drawing, such as preform temperature, translation speed, fiber drawing speed, pressure in the holes, flow rate of inert gas circulating along the preform etc... By selecting suitable sets of parameters we can draw various kinds of holey microstructured and suspended core fibers. Figure 2 shows the pictures of the sections of several MOFs that have been drawn from the preforms obtained using our mechanical drilling technique illustrated Fig. 1.

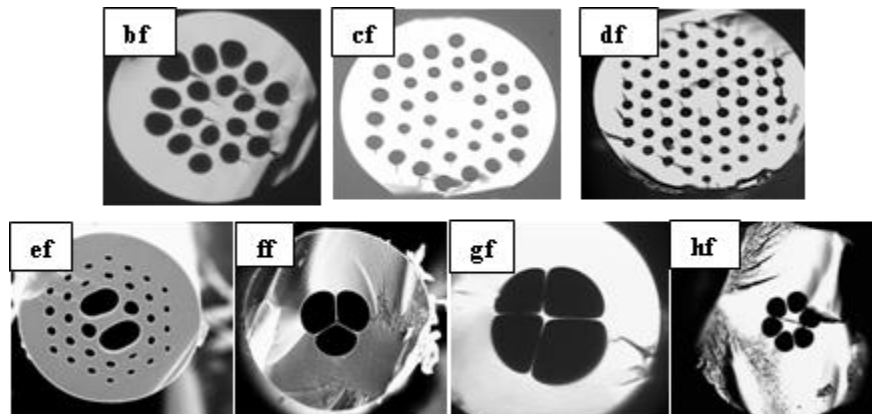


Fig. 2. Geometrical profiles of microstructured optical fibers drawn from preforms depicted in Fig. 1. (bf, cf, df, ef, ff, gf and hf correspond to the preforms b, c, d, e, f, g, h respectively). Depending on fibers, the external diameter varies from 120 μm up to 160 μm .

3. As₂S₃ glass and optical characterizations of As₂S₃ MOFs

3.1 As₂S₃ glass characterizations

We choose As₂S₃ as glass composition because it is hardly crystallizing and exhibits high infrared transparency (up to 10 μm on bulk peaces). This glass presents a good compromise between material infrared transparency and non linear coefficient by comparison with other non oxide glasses (like fluoride glasses), or oxide glasses (such as silicate glasses or heavy oxides glasses) [5,6]. The non linear refractive index n_2 is measured between 3 and 5 10⁻¹⁸ m²/W depending on the wavelength [24,25]. The glass transition temperature is 210 °C, as measured by differential scanning calorimetry (DSC) at the heating rate of 10 °C/min. By comparison with other chalcogenides such as selenides for example (and further more tellurides), we focus in this work on As₂S₃ glass because of its dispersive properties, which are more favorable to the management of the MOFs chromatic dispersion. Indeed, the zero dispersion wavelength (ZDW) of As₂S₃ bulk is at 5 μm, since the ZDW of As₂Se₃ for example is above 6 μm.

We have checked the atomic composition of our glasses. For different samples, deviation of As_xS_{100-x} glass composition is not more than 1-3 atomic % from the stœchiometric one, as measured by energy dispersive spectroscopy (EDS) analysis. The As-S glass composition spreading is due to peculiarity of the glass purification procedure. We did not observe any considerable influence of the glass composition deviations on the fiber optical losses, measured at 1.55 μm using the classical cut-back technique. We have also controlled the composition homogeneity in the same sample by microprobe measurements of three different areas, the middle and both extremities of a glass slide (Table 1). The composition variations remain lower than the resolution of the apparatus and we note that the average composition is close to stœchiometric one, showing a good homogenization during glass synthesis.

Table 1. S and As elemental compositions for three different areas of the same As₂S₃ glass slide (16 mm diameter and 5 mm thickness).

| Elemental Composition (at %) | Zone 1 | Zone 2 | Zone 3 | Average |
|------------------------------|--------|--------|--------|---------|
| S | 60,09 | 60,60 | 60,53 | 60,41 |
| As | 39,91 | 39,41 | 39,47 | 39,59 |

3.2 Optical losses of As₂S₃ single index fibers

In order to check the optical quality of our glasses, we have first measured the losses level of single index fibers using the cut-back technique between 2 and 5 μm with the help of a FTIR spectrometer. Depending of the batches, the minimum of losses is measured between 0.1 dB/m and 0.5 dB/m. For the best attenuation curve we have obtained to date (Fig. 3), the average background level of the losses (≈0.1 dB/m) shows that the material losses contribution induced by our glasses can be pretty low.

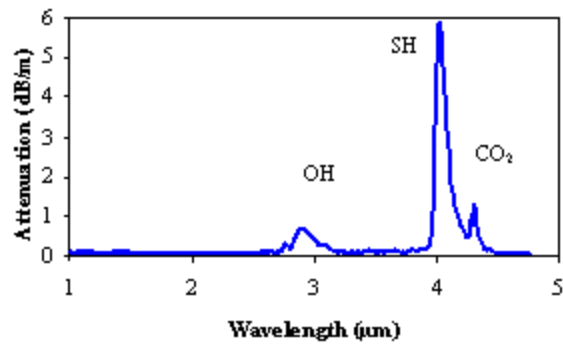


Fig. 3. Attenuation curve of a single index 200 μm outer diameter As_2S_3 optical fiber.

We observe an extrinsic absorption band centered at 4 μm (≈ 6 dB/m) which corresponds to a residual SH pollution of the glass. The extinction coefficient associated to the SH vibration being 2.5 dB/m/ppm [26] at 4 μm , the residual SH content appears to be around 2 ppm. We observe also some residual O-H absorption at 2.9 μm (≈ 0.5 dB/m) and some residual carbon with a CO_2 absorption band at 4.3 μm (≈ 1 dB/m) corresponding to a residual carbon pollution of 60 ppb [21].

3.3 As_2S_3 MOFs linear characterizations

Depending on the preform geometry and of the drawing conditions, various As_2S_3 MOFs can be obtained (Fig. 2), and especially suspended core ones with core diameters around 2 μm (Fig. 2f). Attenuations at 1.55 μm were measured on 20 to 45 m long MOF of this geometry. Actually, losses are located between 0.35 dB/m and 0.7 dB/m depending on the glass quality and microstructure geometry. To our knowledge, these are the lowest attenuations reported to date on chalcogenide based MOFs [27,29]. It is worthy to remind that to ensure accurate core propagation losses measurements in MOF (or even simply double index fiber), the clad must be depleted. In this work, this is systematically done by deposition of an indium/gallium alloy (liquid at room temperature) onto the fibers, thus leading to absorption of the evanescent wave related to clad propagation. In order to verify that the light propagates into the core of our microstructured fibers, we have imaged the output beam intensity distribution using a microscope objective and a CCD camera (Fig. 4).

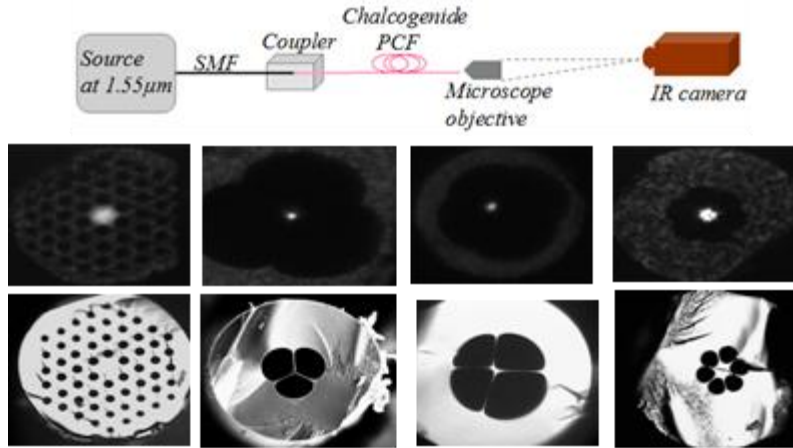


Fig. 4. As_2S_3 MOFs output beam imaging setup.

Several fibers have been tested in that configuration and the beam profiles recorded (Fig. 5.). We know that, due to numerical apertures mismatch and diffraction, the measured profiles do not reflect the propagating modes intensity distribution. However, core propagation is confirmed, and the importance of the clad depletion by means of a metallic coating is illustrated.

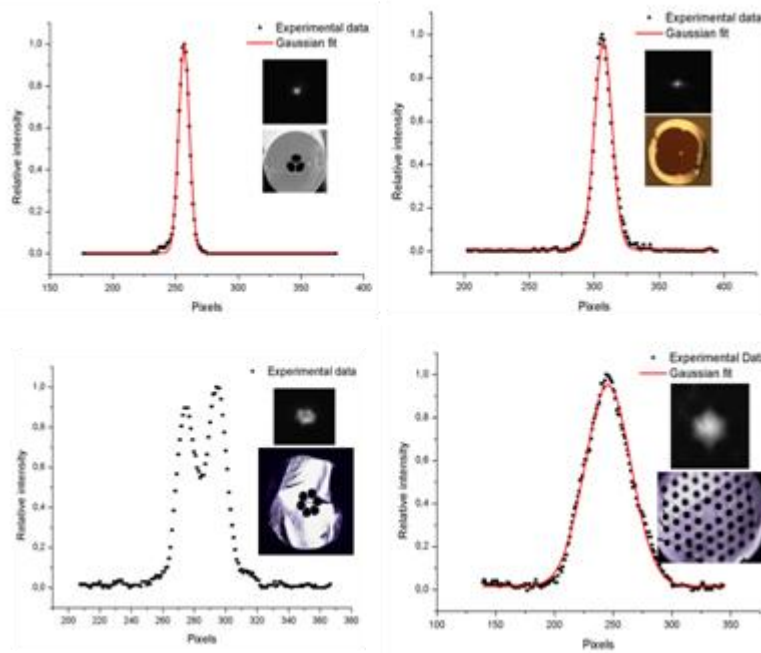


Fig. 5. Mode profiles of some As_2S_3 MOFs using the output beam imaging setup at $1.55\mu m$.

Chromatic dispersion of 50 cm long As_2S_3 MOFs has been measured in the 1200-1750 nm range by the white light interferometry technique [29,30]. The experimental results obtained for several MOFs are presented in Fig. 6. Due to the small experimental measurements range, these results are calculated according to a linear function. However, to estimate the zero dispersion wavelengths (ZDW), numerical simulations have been performed on the basis of the finite element method [29]. For the suspended core fiber with a core diameter of $2\mu m$

(resp. 2.6 μm) the extrapolated ZDW is at 2 μm (resp. 2.2 μm) [29]. They appear strongly shifted towards shorter wavelengths by comparison with the ZDW of the bulk which is located above 5 μm , showing the influence of the geometry, and particularly the core diameter, for optical properties tailoring [29,31].

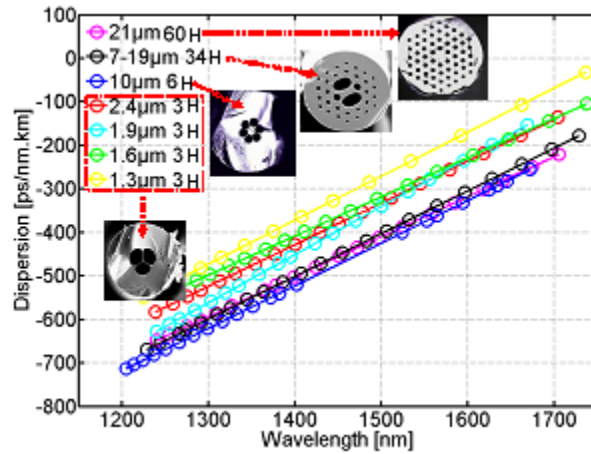


Fig. 6. Chromatic dispersion of suspended core As_2S_3 MOFs with core diameters between 2 μm and 10 μm , and chromatic dispersion of As_2S_3 MOFs with 34 and 60 holes

3.4 As_2S_3 MOFs non linear characterizations

a/ All optical regeneration

We investigate the feasibility of all-optical regeneration in our suspended core chalcogenide MOFs for Telecom applications. More precisely, we design the well-known Mamyshev regenerator based on the self-phase modulation in normal dispersion regime followed by an offset spectral filtering and we characterize its transfer function [32]. In order to obtain a step-like power transfer function we combined 2 meters of chalcogenide fiber with a fiber Bragg grating band pass filter [33,34]. Figure 7 shows the experimental set-up. A mode-locked fiber laser generating 8-ps pulses at a repetition rate of 22-MHz around 1545.7 nm is amplified at an average power of 17 dBm by means of an Erbium doped fiber amplifier (EDFA). A polarization controller (PC) is also used to maximize the self phase modulation effect within the chalcogenide fiber. The signal power is controlled by a variable attenuator and measured by a power meter (PwM) before injection into the As_2S_3 fiber. In order to obtain an efficient coupling between standard fiber and chalcogenide fiber, we inserted a splicing device, which provides only 3 dB of coupling losses. Note that the input standard silica fiber has a microlens at its extremity with a 2.5 μm waist so as to improve the input coupling.



Fig. 7. Experimental set-up of the Mamyshev-based all-optical regenerator.

The output signal is injected at port #1 of the circulator. The output fiber Bragg grating has a full width at half maximum (FWHM) bandwidth of 0.64 nm (80 GHz) and is shifted by 3 nm from the center input signal frequency. The resulting output power is then collected at port

#3 and analyzed by means of a power meter and an optical spectrum analyzer. Figure 8 illustrates the output peak power as a function of the input power. The experimental results are plotted in crosses and black line, while results of numerical simulations are represented by means of a gray line.

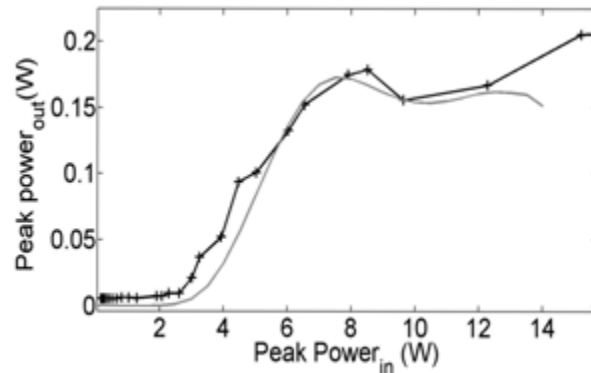


Fig. 8. Transfer function of the Mamyshev regenerator (crosses: experimental results; gray line: simulated results).

The numerical simulations are based on the generalized nonlinear Schrödinger equation and include fiber losses and higher order effects such as Raman scattering and third-order chromatic dispersion [2]. Figure 8 shows a good agreement between experimental and numerical results. We obtained a typical step-like Mamyshev nonlinear transfer function, which exhibits a plateau zone suitable to achieve an efficient regeneration process, especially due to its capacity to equalize pulse-to-pulse peak-power fluctuations [35]. The first part of this nonlinear power transfer function contributes to annihilate the energy contained in the “zeros” bit slots, while the part above the threshold trends to smooth over peak-power fluctuations localized on the “ones” level. Consequently, the ideal working point, localized on the plateau area is then clearly visible around a 10 W peak power. For 40 Gbit/s applications, the suitable average power is thus close to 1.4 W, unfortunately high above the damage threshold of the fiber (around 50 mW). This result clearly shows that these microstructured fibers are not yet ready for all-optical regeneration applications at high bit rates.

b/ Supercontinuum generation

In a previous work [29] by pumping suspended core As_2S_3 MOFs close to $1.55 \mu\text{m}$ with the help of a picoseconds fiber laser, we have obtained more than 200 nm spanning continuum in the infrared, between 1.5 and $1.7 \mu\text{m}$. In this work, we have injected a 400 fs beam at 1557 nm at the repetition rate of 16.75 MHz in 68 cm of an As_2S_3 suspended core fiber with a diameter core of $2.6 \mu\text{m}$ surrounded by three holes (fibers f^f Fig. 2).

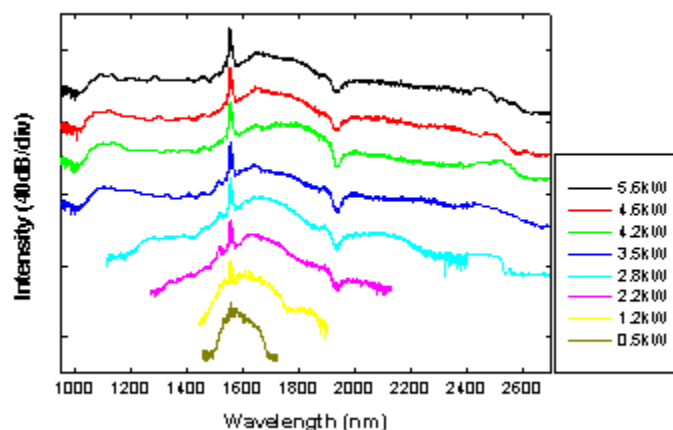


Fig. 9. Experimental spectra recorded for 1557 nm fs pumping of a suspended core As_2S_3 fiber.

This homemade laser source is described in [36]. By varying the input peak power between 0.5 kW and 5.6 kW we have obtained a strong continuous broadening of the initial pulse spanning over more than 1500 nm and extending from about 1 μm until around 2.6 μm in the infrared (Fig. 9). Despite the fact that the pumping of the fiber still occurs in the normal dispersion regime, since the ZDW of this fiber is close to 2.2 μm , these results are of great interest for the further development of efficient light conversion devices in the mid-infrared and of new supercontinuum sources working above 2 μm .

4. Conclusion

We have presented here the recent achievements of our group in the fabrication and optical characterizations of As_2S_3 microstructured optical fibers (MOFs). A mechanical drilling process is used for preforms fabrication, allowing the design of a wide range of chalcogenide microstructured optical fibers. This technique appears to be a relevant alternative to other techniques such as stack and draw or extrusion. We have then drawn MOFs with an efficient tailoring of their optical properties and we have reached low propagation losses and high nonlinear efficiency. As an illustration, the fs pumping of a suspended core MOFs around 1.5 μm leads to a supercontinuum of more than 1500 nm between 1 μm and 2.6 μm . The challenging pumping of these fibers in their anomalous dispersion regime would then lead to new infrared broadband sources.

Acknowledgments

We thank for their supports the Brazilian FAPESP and French CNRS for the fibers drawing collaboration, the Conseil Regional de Bourgogne and the french National Research Agency (ANR CONFIAN).